

Dielectric monitoring of water absorption in glass-bead-filled high-density polyethylene

P. A. M. Steeman*, F. H. J. Maurer* and M. A. van Es

DSM Research BV, PO Box 18, 6160 MD Geleen, The Netherlands

(Received 4 October 1989; revised 28 February 1990; accepted 28 February 1990)

Model composites of spherical glass particles dispersed in a matrix of high-density polyethylene (HDPE) were prepared. Samples of the composite material were, after careful drying, exposed to several relative humidities at room temperature. The dielectric properties and the mass gain of the composite samples were monitored during the water absorption from the environment. The dielectric measurements covered the frequency range from 0.1 Hz to 50 kHz. A theoretical model for the dielectric properties of composites with an interlayer describes the detected dielectric loss processes due to the electrically conducting layer of adsorbed water at the filler-matrix interface. A quantitative relationship between the amount of adsorbed water and the frequency of maximum dielectric loss can be established by taking into account the thickness dependence of the conductivity of the interfacial water layer.

(Keywords: dielectric constant; composite; glass-filled polymer; interfacial water; interlayer model)

INTRODUCTION

An increase of the dielectric constant ϵ' and of the loss index ϵ'' of composites after absorption of water has been reported by several authors¹⁻⁸. The considered composites consist of a matrix material with filler particles or fibres dispersed in it. The dielectric loss effects seem to be dominant specifically at low frequencies and are often related to the absorption of water into the interfacial regions of filler/fibre and matrix. Plueddemann⁹ states that, even if a glass-based composite is prepared with perfectly dry glass, water will be able to reach the interface by diffusion through the polymer. Moreover, any imperfections or microcracks in the composite formed through stresses generated by differential shrinkage allow water to get to the interface even more rapidly. The composite can be considered as a three-phase system in which the adsorbed water forms an interlayer between the filler particles and the matrix material. This conducting interlayer between the glass filler and the matrix material gives rise to an interfacial dielectric loss process, which can be detected by audiofrequency dielectric measurement systems.

Bánhegyi and Karasz¹⁻³ detected a low-frequency, low-temperature loss process in CaCO₃-filled polyethylene due to adsorbed water. The high-frequency dielectric constant can be described reasonably well by the models proposed for heterogeneous mixtures, but the frequency-dependent dielectric losses cannot be interpreted on the basis of a simple interfacial loss mechanism. The 'universal response theory' offers a good description of the detected loss processes, but because of its universality it is unable to describe the effects in terms of structural characteristics.

The conductivity of carbon-fibre-filled epoxy resins in a direction normal to the fibre alignment decreases with increasing amount of adsorbed water according to Bunsell⁴. This is understood to be caused by the swelling

of the composite due to the water uptake. By contrast, glass-fibre-filled epoxy resins show a large enhancement of the electrical conductivity above a certain threshold level of adsorbed water. Possibly a network of free water molecules, allowing electrical conduction, is built up. Moreover, the interface between filler and matrix accounts for the strong dielectric loss effects during the water absorption process.

Cotinaud, Bonniau and Bunsell⁵ observed three mechanisms of water absorption. The first mechanism is simple reversible Fickian diffusion of water molecules into the matrix, causing a slight increase of the sample dielectric constant and dielectric loss. The second mechanism is observed at higher humidity levels, where a large increase of the dielectric losses together with electrical conduction occur due to a redistribution and regrouping of the adsorbed water molecules. The third mechanism, which is only seen on immersion, is transport of water along microcracks in the matrix material through capillary action. The electrical conductivity of the composite increases sharply due to this process.

Reid and Lawrence⁶ studied the dielectric relaxation behaviour of glass-epoxy composites and suggested three modes of moisture interaction. At low moisture concentration they detect a decreased dielectric loss intensity, which is probably due to compensating dipole pairing. At higher moisture concentrations the increased loss intensity as detected suggests co-relaxation of the water dipoles with the segments on which they adsorb. At high moisture concentrations the building-up of formations of colloidal or weakly adsorbed water may be responsible for a separate loss process.

Woo and Piggot⁷ state that the adsorbed water in glass-epoxy composites is concentrated in the interfacial regions, which are interconnected by disc-shaped water clusters providing conducting paths.

Paquin, St-Onge and Wertheimer⁸ studied the dielectric properties of polymer composites containing plasma-treated mica. The detected low-frequency dispersion can

* To either of whom correspondence should be addressed

be ascribed to the intrinsic dispersive properties of the mica filler. However, the broad audiofrequency loss peak is due to Maxwell–Wagner–Sillars loss peaks associated with water adsorbed at the filler surface.

Dielectric experiments as reported in the literature are often difficult to interpret because of the complexity of the systems considered. Most authors assume that the absorbed water is concentrated in the interfacial regions between filler/fibre and matrix. However, no clear physical picture of the dielectric effects of a conducting interfacial layer in composites is obtained.

We therefore studied the influence of an absorbed water interlayer at a filler–matrix interface by monitoring the water absorption of glass-bead-filled high-density polyethylene (HDPE) composites by dielectric spectroscopy. The water uptake by such composites is only due to the adsorption of water molecules at the filler (glass sphere) surface. A set of dried samples was, at room temperature, exposed to environments with controlled relative humidity. The relative mass gain and the dielectric properties of these samples were monitored during the water uptake from the environment. In this work we present the results of the experimental dielectric work on the water absorption of these composites and compare them with recent theoretical developments^{10,11}.

MATERIALS

Composites of glass-sphere-reinforced high-density polyethylene (HDPE) were prepared as follows. After milling 122.58 g of HDPE at 170°C on a Schwabenthan Polymix 80T open two-roll mill for 4 min, 78.57 g of glass spheres were added. Milling was continued for 12 min, after which the composite material was compression moulded into 0.16 cm thick plates under standard conditions at 190°C. Standard conditions include a pressure of 300 kg cm⁻² and a cooling rate of 40°C min⁻¹. Samples with dimensions 75 × 75 × 1.6 mm³ were cut from these compression-moulded plates.

The linear polyethylene (Stamylan 9089F, DSM) was a high-purity-grade HDPE with a density of 963 kg m⁻³ at 23°C, $M_w = 60$ kg mol⁻¹ and a melt flow index of 8 g/10 min. The glass spheres (Potters Industries, type NJ 0-66-810), with a density of 2490 kg m⁻³, had an average particle size of 10–13 µm. Brunauer–Emmett–Teller (BET) measurements, in which the amount of Kr gas adsorbed at the glass surface at 77 K was determined, indicate an average surface area of 5.9 m² g⁻¹ of the filler particles. By milling the mentioned amounts of HDPE and glass particles, a filler volume fraction of 20% was obtained.

The glass particle size distribution was measured from light scattering experiments on a dispersion of the glass spheres in water using a Malvern Particle Sizer model 2600D. Table 1 contains the mean cumulative weight fraction of the glass particles with diameter larger than a given range as a function of the particle diameter in micrometres.

Before milling, the glass spheres were treated to leach ions from their surfaces. This was accomplished by washing 300 g of glass spheres for 17 h in a 0.5 N HCl solution, followed by repeated washing in demineralized water and drying in a furnace at 110°C. Finally, the glass spheres were brought into 0.5 litre of acetone followed by drying for two days in a furnace at 110°C.

EXPERIMENTAL

Five closed containments partially filled with saturated aqueous salt solutions were prepared to study the water absorption of the glass-bead-filled HDPE composites from environments with different constant relative humidities. Table 2 summarizes the salt types used and the relative humidities (RH) above the salt solution at room temperature (20°C). A dry atmosphere is obtained in a containment partially filled with Mg(ClO₄)₂, while a saturated (RH 100%) environment is obtained above demineralized water.

After drying for about one year in the dry air containment (No. 1) the masses and the dielectric properties of the samples were measured. The experiment was started by inserting the sample plates in containments 2–7 and thus exposing them to a controlled relative humidity environment.

The dielectric properties of the samples were monitored by inserting the sample plates in a Balsbaugh three-terminal parallel-plate capacitor and measuring the complex admittance of the cell with a Solartron Frequency Response Analyser type 1250 and an electrometer built by TNO (Dutch Organization for Applied Scientific Research), controlled by a HP 9816 computer. The computer converted the admittance data to the sample dielectric constant ϵ' and loss index ϵ'' . Dielectric measurements were made in the frequency domain from 0.1 Hz to 50 kHz with 10 frequency steps per decade. The amplitude accuracy of the system is better than 0.3% while the phase accuracy is about 0.03°.

Table 1 The diameter distribution of the glass filler particles as obtained from light scattering experiments

Band number	Band boundaries (µm)		Mean cumulative weight above (%)	Standard deviation
	Lower	Upper		
1	1.22	1.52	95.3	0.0
2	1.52	1.90	92.3	0.0
3	1.90	2.39	89.3	0.0
4	2.39	3.04	86.7	0.0
5	3.04	3.87	81.4	0.0
6	3.87	4.96	75.6	0.1
7	4.96	6.37	65.7	0.3
8	6.37	8.19	55.8	0.2
9	8.19	10.53	47.4	0.2
10	10.53	13.58	27.5	0.4
11	13.58	17.70	3.0	0.1
12	17.70	23.69	0.1	0.1
13	23.69	33.67	0.1	0.1
14	33.67	54.94	0.1	0.1
15	54.94	118.43	0.1	0.1

Table 2 Salt solutions used for obtaining the controlled relative humidity environments

Containment	Salt/solution	RH at 20°C (%)
1	Dry Mg(ClO ₄) ₂	0
2	Saturated LiCl	14
3	Saturated CaCl ₂	31
4	Saturated Na ₂ Cr ₂ O ₇	51
5	Saturated NaCl	75
6	Saturated KCl	87
7	Demineralized water	100

The sample masses were measured on a Mettler AE240 balance, with a resolution of 0.1 mg.

The dielectric properties and the masses of the samples were monitored 11 times during about 170 days. Water uptake or loss during a measurement cycle, which takes about 15 min, can be neglected.

THEORETICAL

The water absorption of the composites

The water absorption of materials can often be described by the classical model for the absorption of a single free phase into a continuum. This model is based on the diffusion theory by Fick. The water absorption of the sample results from the water concentration gradient. The mass gain due to single-phase diffusion can be described with only two parameters, the diffusion coefficient D and the relative mass gain at saturation M_m (%). The water absorption rate of a sample plate also depends on the sample thickness h .

The relative mass gain ΔM (%) as a function of time t is given by¹²:

$$\Delta M = M_m \left[1 - \frac{8}{\pi^2} \sum_{n=0}^{\infty} \frac{1}{(2n+1)^2} \exp\left(-\frac{Dt}{h^2} \pi^2 (2n+1)^2\right) \right] \quad (1)$$

This relation simplifies for short time intervals ($Dt/h^2 < 0.05$) to a linear relationship between the relative mass gain and the square root of the diffusion time¹²:

$$\Delta M = M_m \frac{4}{\pi^{1/2}} \left(\frac{Dt}{h^2} \right)^{1/2} \quad (2)$$

At longer experimental times ($Dt/h^2 \gg 0.05$) the sample becomes saturated with water and relation (1) can be simplified to:

$$\Delta M = M_m \left[1 - \frac{8}{\pi^2} \exp\left(-\frac{Dt}{h^2} \pi^2\right) \right] \quad (3)$$

In view of the initial linear relationship between the amount of water absorbed by the samples and the square root of the absorption time, the dielectric experiments were performed at time intervals in a quadratic series starting from time zero.

The dielectric properties of the composites

Analogous to the description of the shear modulus¹³, the bulk modulus¹³ and the thermal expansivity¹⁴ of particulate-filled polymers with an interfacial layer, we derived the dielectric constant of a composite with interlayer as a function of the volume fractions and the properties of the filler, the interlayer and the matrix¹⁰. The resulting static model was extended to a conductive interlayer and to oscillatory fields, the latter extension being made using the correspondence principle.

The basic derivations were made by assuming a representative volume element that consists of a filler particle surrounded by an interlayer, embedded in matrix material and finally enveloped by composite material. The volume fraction of the filler is ϕ_f , that of the interlayer is ϕ_l and that of the matrix is ϕ_m . Application of an external homogeneous electric field on the representative volume element, with the imposed condition that the electric potential and the normal component of the

dielectric displacement are continuous, yields the following equations for the relative static dielectric constant ϵ_c of the composite¹⁰:

$$\epsilon_c = \frac{\epsilon_f \phi_f + \epsilon_l \phi_l R + \epsilon_m \phi_m S}{\phi_f + \phi_l R + \phi_m S} \quad (4)$$

with:

$$R = \frac{2\epsilon_l + \epsilon_f}{3\epsilon_l} \quad (5)$$

$$S = \frac{(2\epsilon_l + \epsilon_f)(2\epsilon_m + \epsilon_l) - 2d(\epsilon_l - \epsilon_m)(\epsilon_l - \epsilon_f)}{9\epsilon_m \epsilon_l} \quad (6)$$

$$d = \frac{\phi_f}{\phi_l + \phi_f} \quad (7)$$

where ϵ_i with $i = c, f, l, m$ stands for the static dielectric constant of the composite, the filler, the layer or the matrix, respectively.

Using the correspondence principle, equation (4) can be extended to oscillatory fields by replacing the static dielectric constants ϵ_i by the complex dielectric constants $\epsilon_i^*(\omega)$, for $i = c, f, l, m$.

The complex dielectric constant $\epsilon^*(\omega)$ of a material is defined according to relation (8), where ω is the angular frequency:

$$\epsilon^*(\omega) = \epsilon'(\omega) - i\epsilon''(\omega) \quad (8)$$

and in which $\epsilon'(\omega)$ is the frequency-dependent dielectric constant of the material and $\epsilon''(\omega)$ the frequency-dependent loss index of the material.

When a composite contains conducting materials, the complex dielectric constants $\epsilon^*(\omega)$ in relation (4) have to be replaced by the generalized complex dielectric constants $\underline{\epsilon}(\omega)$, which also include the complex conductivity $\sigma^*(\omega)$ of the materials. The relative generalized complex dielectric constant $\underline{\epsilon}^*(\omega)$ of a material is defined as¹⁵:

$$\underline{\epsilon}^*(\omega) = \epsilon^*(\omega) + \frac{\sigma^*(\omega)}{i\omega\epsilon_{vac}} \quad (9)$$

in which $\epsilon^*(\omega)$ is the complex relative dielectric constant of the material, $\sigma^*(\omega)$ is the complex conductivity of the material, and ϵ_{vac} is the permittivity of vacuum, which equals 8.82 pF m^{-1} .

We assume the interlayer to be conductive with a frequency-independent conductivity and that the filler, the interlayer and the matrix have frequency-independent dielectric constants. In this case, for small layer volume fractions, i.e. $\phi_l \ll \phi_f$, and if, in the frequency range considered, the absolute dielectric constant of the layer is much smaller than the layer conductivity divided by the angular frequency, i.e. $\epsilon_l \ll \sigma_l/\omega$, the generalized form of relation (4) reduces to a Debye-type relaxation¹⁰:

$$\epsilon_c^*(\omega) = \epsilon_\infty + \frac{\epsilon_0 - \epsilon_\infty}{1 + i\omega\tau} \quad (10)$$

with:

$$\epsilon_0 = \epsilon_m \frac{1 + 2\phi_f}{1 - \phi_f} \quad (11)$$

$$\epsilon_\infty = \epsilon_m \frac{(\epsilon_f + 2\epsilon_m) + 2(\epsilon_f - \epsilon_m)\phi_f}{(\epsilon_f + 2\epsilon_m) + (\epsilon_f - \epsilon_m)\phi_f} \quad (12)$$

$$\tau = \frac{\phi_f}{1 - \phi_f} \frac{3\epsilon_{vac}}{2\sigma_1\phi_l} [(\epsilon_f + 2\epsilon_m) - (\epsilon_f - \epsilon_m)\phi_f] \quad (13)$$

where ϵ_0 is the low-frequency limit of the composite dielectric constant, ϵ_∞ is the high-frequency limit of the composite dielectric constant and τ is the retardation time of the loss process.

According to relation (11), the low-frequency limit of the dielectric constant ϵ_0 is only dependent on the matrix dielectric constant ϵ_m and the filler volume fraction Φ_f . Owing to the conductive interlayer on the filler surface, the electric field is screened off from the filler particles, as in the case of a composite of entirely conductive particles.

Relation (12) for the high-frequency limit of the composite dielectric constant equals the Rayleigh formula¹⁶ for a two-phase composite of dispersed spheres.

The retardation time of the predicted dielectric loss process is essentially inversely proportional to the product of the interlayer volume fraction and the interlayer conductivity, as can be seen from relation (13).

RESULTS AND DISCUSSION

The water absorption

Figure 1 shows the measured relative mass gain as a function of time for the samples in the 14%, 31%, 52%, 75%, 87% and 100% relative humidity environments. The numbers above the RH 100% curve refer to the measurement cycles. We assume that the samples are in equilibrium with their environment after 169 days. We therefore use the relative mass gain at this time as an approximation of the equilibrium relative mass gain. The relative mass gain in equilibrium is listed as a function of the environmental humidity in column 2 of Table 3. The mass gain does not show the expected direct proportionality to the humidity but can be described by an exponential function:

$$M_m = 0.0188(RH)^{0.575} \quad (14)$$

A relation of the same type was obtained by Woo and Piggot⁷ for glass-fibre-filled resins with an exponential factor of 1.4:

$$M_m = 0.0044(RH)^{1.40} \quad (15)$$

Using formula (2) the diffusion coefficient D can be

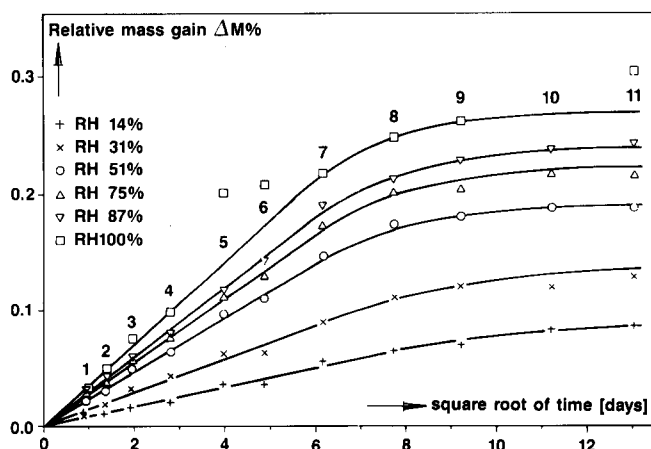


Figure 1 The relative mass gain of the samples as a function of the square root of time for the samples in the 14%, 31%, 51%, 75%, 87% and 100% relative humidity environments at 23°C. The numbers of the measurement cycles are indicated above the RH 100% curve

Table 3 The equilibrium relative mass gain of the samples and the calculated diffusion coefficients of water in the HDPE-glass composites as a function of the environmental relative humidity

RH (%)	Mass gain (%)	$D \times 10^{14}$ (m ² s ⁻¹)
14	0.086	4.0 ± 0.4
31	0.134	5.1 ± 0.3
51	0.187	6.8 ± 0.3
75	0.222	7.2 ± 0.2
87	0.240	8.3 ± 0.2
100	0.269	9.5 ± 0.6

calculated from the initial slope of the mass gain versus time curve and the approximate equilibrium mass gain of the samples. Table 3 also contains these calculated diffusion coefficients as a function of the relative humidity of the environment. It appears that the diffusion coefficient of water in the composite samples depends on the relative humidity of the environment to which the samples were exposed.

Both the non-linear equilibrium water uptake and the humidity-dependent diffusion coefficient of the samples suggest that the water uptake of the HDPE matrix material is not the dominant water absorption process in these glass-bead-filled HDPE composites. Rather, the adsorption of water at the glass (filler) surface seems to be the most important absorption mechanism in these composites.

Though the Fickian absorption theory is not applicable to this type of diffusion process, we reinserted the calculated diffusion coefficients into relation (3). We calculated that the samples had reached 97% (in the case of the RH 14% sample) to 99% (in the case of the RH 100% sample) of their equilibrium water uptake.

The dielectric properties of the composite samples

Figures 2–7 show the dielectric constant ϵ' and loss index ϵ'' as functions of frequency, measured during the 11 measurement cycles for the samples in the 14%, 51% and 100% relative humidity environments. The numbers next to the curves are the measurement cycle numbers and correspond to the numbers in Figure 1.

Measurement cycle 0 shows the dielectric properties of the carefully dried samples before they were exposed to the different relative humidities. All samples have the same, frequency-independent, dielectric constant of about 3.0 and show no dispersion in the experimental frequency window between 0.1 Hz and 10 kHz. Only at low frequencies ($f < 10$ Hz) can the onset of a dielectric loss process be detected.

After the samples had been exposed to the different relative humidities for about 37 days (cycle 7) most of them showed a dielectric loss peak in the experimental frequency window. The frequency of maximum dielectric loss shifts to higher frequencies with increasing humidity of the environment. For all samples the high-frequency limit of the dielectric constant equals about 3.0, the same value as measured for the dried samples.

The dielectric properties after 169 days exposure, the time by which the samples were assumed to be in equilibrium with their environment (cycle 11), show the same features as the non-equilibrium measurements (cycles 7–10). However, the frequencies of maximum dielectric loss have shifted to higher values while the loss

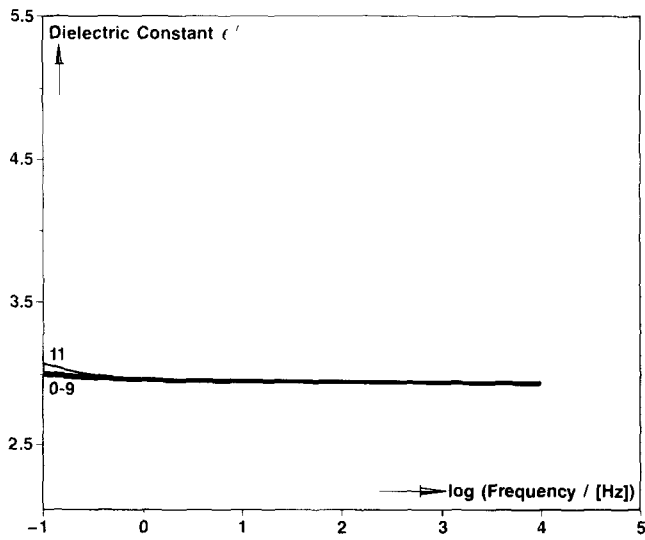


Figure 2 Experimental data of the dielectric constant as a function of frequency for the composite sample in the RH 14% environment at 23°C. The numbers next to the curves refer to the measurement cycles

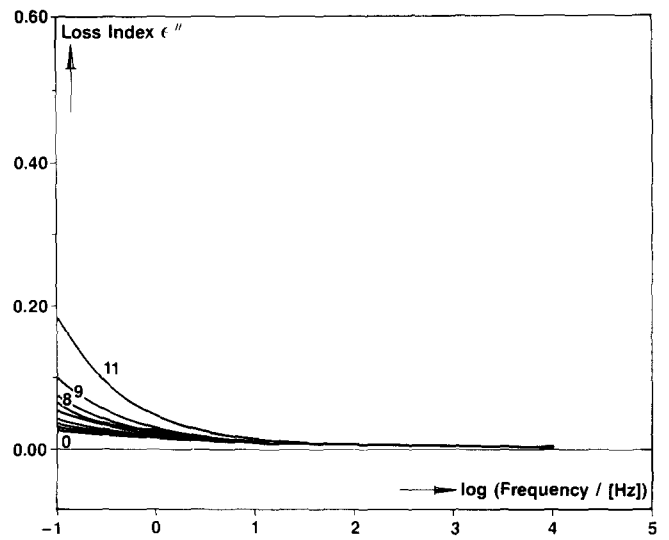


Figure 3 Experimental data of the dielectric loss index as a function of frequency for the composite sample in the RH 14% environment at 23°C. The numbers next to the curves refer to the measurement cycles

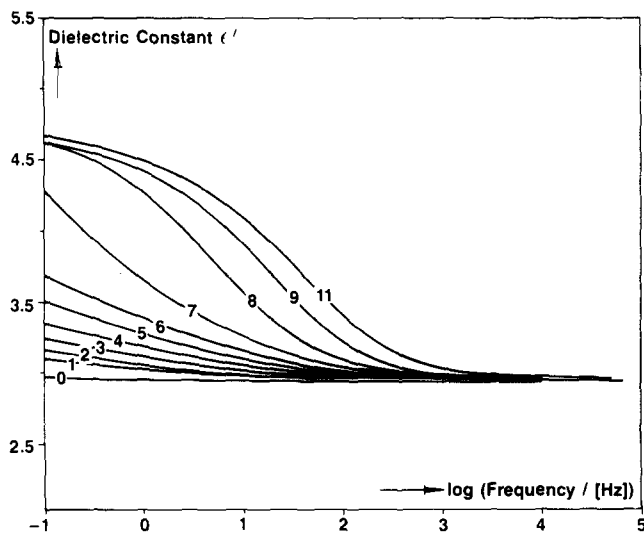


Figure 4 Experimental data of the dielectric constant as a function of frequency for the composite sample in the RH 51% environment at 23°C

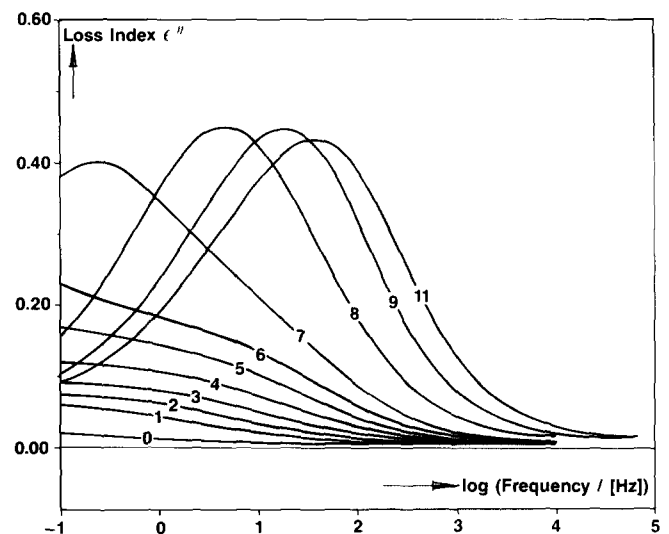


Figure 5 Experimental data of the dielectric loss index as a function of frequency for the composite sample in the RH 51% environment at 23°C

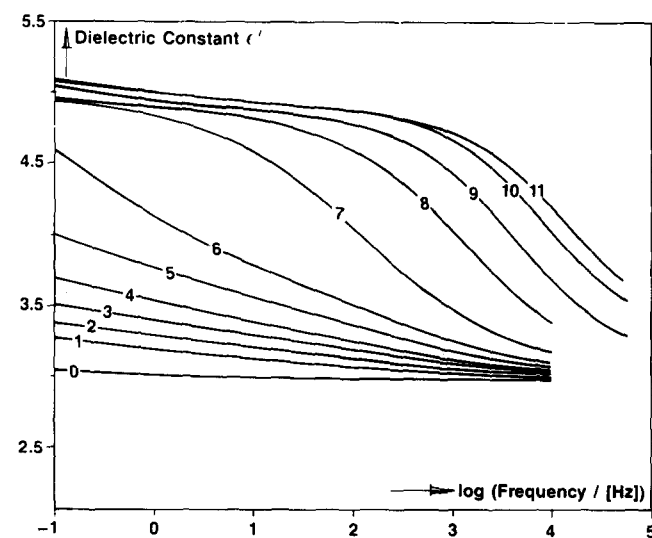


Figure 6 Experimental data of the dielectric constant as a function of frequency for the composite sample in the RH 100% environment at 23°C

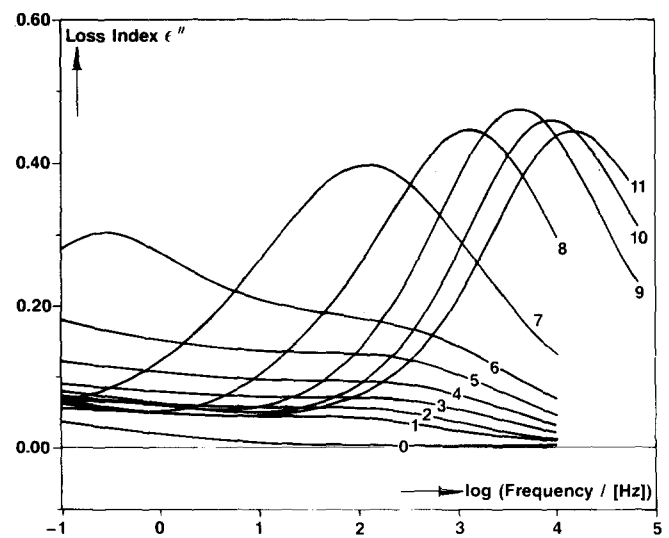


Figure 7 Experimental data of the dielectric loss index as a function of frequency for the composite sample in the RH 100% environment at 23°C

peaks have sharpened. Under the same experimental conditions no dielectric losses were detected for unfilled HDPE samples.

The observed loss peaks are much broader than the predicted Debye-type peaks. In polymeric materials broader peaks are nearly always observed. The peak broadening is a result of a distribution of retardation times. This distribution may in our case have been caused by two effects. First, the distribution in particle size of the dispersed glass spheres results in a range of layer volume fractions through the sample. Secondly, in non-equilibrated samples the inhomogeneous water absorption through the sample will also give rise to a distribution of layer volume fractions through the sample. As can be seen from relation (13), both mechanisms will result in a range of retardation times and thus in broadened peaks. We do indeed observe smaller loss peaks for the equilibrated samples (series 11) than for the non-equilibrium samples.

The Cole–Cole dispersion relation (16) can be used instead of the Debye relation (10) to describe the observed broader loss peaks. This relation incorporates a symmetric broadening of the loss curves, which is described by the broadening parameter α ($0 < \alpha < 1$ and $\alpha = 1$ for a Debye loss process). The Cole–Cole relation is given by¹⁷:

$$\varepsilon^*(\omega) = \varepsilon_\infty + \frac{\varepsilon_0 - \varepsilon_\infty}{(1 + i\omega\tau)^\alpha} \quad (16)$$

In this formula ε_0 , ε_∞ and τ are, as in relation (10), the static dielectric constant, the high-frequency limit of the dielectric constant and the retardation time of the loss process, respectively.

Table 4 summarizes the Cole–Cole parameters ε_0 , ε_∞ , τ and α that were obtained from a least-squares fit of the experimental dielectric data of the equilibrated glass–HDPE samples to the Cole–Cole relation (16). Both the experimental values of the dielectric constant and the loss index were used as input for a parameter estimation program, based on a Newtonian iteration technique, in order to obtain the best possible fit. From the curves of the equilibrated samples one can see the onset of an additional very low-frequency (less than 5 Hz) dispersion, which appears besides the predicted interfacial loss process. This dispersion may result from polarization effects at the surface or some other as yet unknown effects. As a result, the low-frequency permittivity increases with decreasing frequency. The effect is most pronounced in the samples in the higher relative humidity environments. We therefore omitted the dielectric data below 5 Hz from the Cole–Cole parameter fit.

The HDPE as used has a frequency-independent dielectric constant ε' of 2.4 and shows no dielectric loss in the experimental frequency window. For the glass filler particles we assume also a frequency-independent dielectric constant of about 5.5 and no dielectric loss. Using these values we obtain from the interlayer model the value $\varepsilon_0 = 4.20$ (equation (11)) for the low-frequency limit of the dielectric constant of the composite, and for the high-frequency limit $\varepsilon_\infty = 2.86$ (equation (12)). The broadening parameter $\alpha = 1$, in accordance with a Debye-type retardation. The experimentally obtained high-frequency limits of the composite dielectric constant agree fairly well with the theoretically calculated value, except for some small deviations. The experimental low-frequency limits of the composite dielectric constant are about 0.2 to 0.7 higher than the theoretically calculated value.

The (water) layer volume fraction Φ_1 is related to the relative mass gain ΔM of the composite (in per cent) via the composite density ρ_{comp} , which is 1260 kg m^{-3} , and the density of water ρ_w . The layer volume fraction can be calculated from:

$$\Phi_1 = (\rho_{\text{comp}}/\rho_w)(\Delta M/100) = 1.26 \times 10^{-2} \Delta M \quad (17)$$

If the layer conductivity were constant, independent of the amount of absorbed water, then the retardation time of the loss process would be inversely proportional to the amount of water absorbed, according to relation (13). However, the retardation times τ obtained from the Cole–Cole parameter fitting to the experimental data depend very strongly, more than inversely proportionally, on the amount of absorbed water. This can only be explained if the water layer conductivity σ_1 depends on the layer thickness. It is therefore important to obtain insight into the conductivity of thin water layers on glass surfaces as a function of the layer thickness.

Fripiat¹⁸ studied the conductivity of thin water films on powdered glass. At coverages greater than one molecular layer the conductivity of the water layer is an exponential function of the layer thickness. The layer conductivity is mainly cationic and arises from the electric-field-driven transfer of metal cations through the water layer. The conductivity σ ($\Omega^{-1} \text{ m}^{-1}$) can be described by the formula:

$$\sigma = \sigma_0 \exp(C\theta) \quad (\text{for } \theta > 1) \quad (18)$$

where σ_0 and C are constants and θ is the surface layer coverage ($\theta = 1$ for a monomolecular layer of water) of the glass particles.

In our case the water layer thickness t_1 (m) is directly proportional to the amount of water absorbed by the

Table 4 Cole–Cole parameters fitted for the equilibrated samples

RH (%)	ε_0	ε_∞	τ (s)	α
14 ^a	4.70 ± 0.10	2.95 ± 0.05	$(1.83 \pm 0.1) \times 10^{-1}$	0.72 ± 0.05
31	4.70 ± 0.05	2.95 ± 0.05	$(1.75 \pm 0.1) \times 10^{-1}$	0.65 ± 0.02
51	4.49 ± 0.05	2.95 ± 0.05	$(4.40 \pm 0.2) \times 10^{-3}$	0.66 ± 0.02
75	4.53 ± 0.05	2.98 ± 0.05	$(3.06 \pm 0.2) \times 10^{-4}$	0.61 ± 0.02
87	4.70 ± 0.05	2.93 ± 0.05	$(1.60 \pm 0.1) \times 10^{-4}$	0.55 ± 0.02
100	4.90 ± 0.05	3.18 ± 0.05	$(1.03 \pm 0.1) \times 10^{-5}$	0.60 ± 0.02

^aThe data for the RH 14% sample were obtained by a special measurement technique using a 0.01 Hz square-wave excitation followed by Fourier analysis of the response and subsequent Cole–Cole parameter fitting

composite and can be calculated from:

$$t_1 = \theta t_{\text{mono}} = \frac{(\Delta M/100)}{A_f \rho_w} = \frac{10^{-8} \Delta M}{A_f} \quad (19)$$

where ΔM is the relative mass gain of the composite (in per cent), A_f is the filler surface area (in m^2 per g of composite) and ρ_w is the density of water (in g m^{-3}). The average surface area of the glass particles as determined from BET measurements being $A = 5.9 \text{ m}^2 \text{ g}^{-1}$ and the filler mass fraction being $w_f = 0.39$, the filler surface area per gram of composite amounts to $A_f = 2.30 \text{ m}^2 \text{ g}^{-1}$. The thickness of a monomolecular layer of water molecules t_{mono} is about 3.0 \AA according to Fripiat¹⁸.

By combining the relations (13) and (17)–(19) we can express the frequency (Hz) of maximum dielectric loss ($f_{\text{max}} = 2\pi/\tau$) as a function of the relative mass gain ΔM of the composite as follows:

$$f_{\text{max}} = f_0 (\Delta M / \Delta M_0) \exp(\Delta M / \Delta M_0) \quad (20)$$

where f_0 and ΔM_0 are constants representing a characteristic frequency and mass gain, respectively.

With a parameter estimation computer program based on a Newtonian iteration technique, we fitted the parameters f_0 and ΔM_0 to the experimentally obtained equilibrium mass gain and frequency of maximum dielectric loss of the samples. The fitted parameter values are:

$$\begin{aligned} f_0 &= (6.1 \pm 0.5) \times 10^{-6} \quad (\text{Hz}) \\ \Delta M_0 &= (1.4 \pm 0.1) \times 10^{-2} \quad (\%) \end{aligned} \quad (21)$$

In Figure 8 the logarithm of the frequency of maximum dielectric loss is plotted as a function of the relative mass gain due to water absorption. All dielectric measurements where a loss peak was obtained in the experimentally accessible frequency window are included in the figure. The shifting of the loss peaks with increasing water uptake is clearly visible and occurs along nearly straight lines.

The broken curve is the theoretical curve according to relation (20) using the fitted parameters. The results for all samples lie close to this line. In the mass gain interval from 0.1% to 0.3% as studied, a linear relation between the logarithm of the loss peak frequency and the water

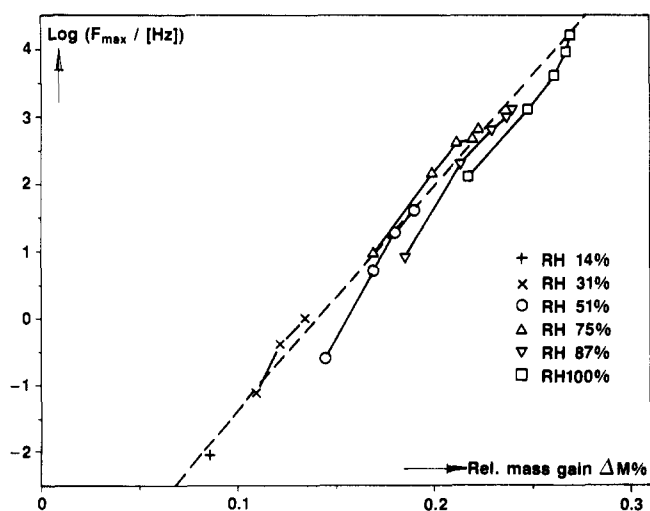


Figure 8 The logarithm of the frequency of maximum dielectric loss plotted against the relative mass gain (in per cent) of the samples for all measurements where a loss peak is detected

Table 5 The surface layer coverage θ and the layer conductivity σ of the equilibrated samples

RH (%)	θ	σ ($\Omega^{-1} \text{ m}^{-1}$)
14	1.25	2.6×10^{-9}
31	1.94	7.2×10^{-8}
51	2.71	2.9×10^{-6}
75	3.22	3.2×10^{-5}
87	3.48	1.1×10^{-4}
100	3.90	8.4×10^{-4}

uptake is obtained. This shows that the shifting of the frequency of maximum dielectric loss due to additional water uptake is mainly governed by the increase of the layer conductivity with increasing layer thickness via the exponential term in relation (20). The layer volume fraction (the pre-exponential ΔM term) plays a minor role in this shifting process.

Using the relations (13) and (17)–(19), relation (20) can be transposed into a relation for the layer conductivity σ_1 ($\Omega^{-1} \text{ m}^{-1}$) as a function of the surface coverage θ of the glass filler particles:

$$\sigma_1 = (6.7 \pm 0.5) \times 10^{-12} \exp[(4.8 \pm 0.5)\theta] \quad (22)$$

Table 5 contains the surface layer coverage θ calculated from relation (19) and the layer conductivity σ calculated from relation (22) of the equilibrated samples for all relative humidities used. The bulk conductivity of pure water at room temperature amounts to about $5 \times 10^{-6} \Omega^{-1} \text{ m}^{-1}$. As can be seen from Table 5 the conductivity of the water interlayer at low surface coverages is less than the conductivity of pure bulk water. This may be due to an electrical double-layer potential in the interlayer, which hinders ionic movement. At higher surface coverages the conductivity exceeds the conductivity of pure water, probably due to conduction by metal cations dissolved from the glass surface. From data reported by Fripiat¹⁸ the following equation can be derived for the water layer conductivity σ ($\Omega^{-1} \text{ m}^{-1}$):

$$\sigma = (0.7 \pm 0.3) \times 10^{-16} \exp[(16.1 \pm 0.5)\theta] \quad (23)$$

Fripiat states that the free surface of the glass particles as determined from BET measurements is too low. Some very tiny channels in the porous glass surface cannot be entered by the krypton gas atoms, while they can be entered by water molecules. He therefore uses an adapted larger value for the surface area, which is responsible for the larger exponential factor.

Moreover, he used a different type of glass (powdered window glass) and did not apply an acid treatment to leach ions from the surface as we did. Both differences may account for the different coefficients in the equations (22) and (23).

CONCLUSIONS

When dried samples of a glass-bead-filled HDPE are exposed to a humid environment, a mass gain due to water absorption can be clearly observed. The water diffusion coefficient increases with increasing humidity of the environment in which the samples are stored. The saturation water uptake appears to be less than directly proportional to the humidity. The adsorption of water molecules at the glass filler surface is probably the dominating process in the water uptake of the composites.

The theoretically predicted dielectric loss effects due to a conducting water interlayer are present in all samples. The peak of the loss process is broader than the predicted Debye-type peak but can be described well using the Cole–Cole relation. This peak broadening is probably caused by both the filler particle size distribution and the initially inhomogeneous water uptake through the samples. The position of the loss peak on the frequency axis can be quantitatively described if the thickness dependence of the conductivity of the water interlayer is taken into account. In the studied mass gain range the layer conductivity is an exponential function of the amount of water absorbed. This dependence governs the peak shifting along the frequency axis. The conductivity of the thinnest water layers is much less than the conductivity of pure water.

REFERENCES

- 1 Bánhegyi, G. and Karasz, F. E. *J. Polym. Sci.* 1986, **24**, 209
- 2 Bánhegyi, G. and Karasz, F. E. *Colloid Polym. Sci.* 1987, **265**, 394
- 3 Bánhegyi, G., Hedvig, P. and Karasz, F. E. *Colloid Polym. Sci.* 1988, **266**, 701
- 4 Bunsell, A. R. *Reinforced Plast.* 1984, **3**, 1
- 5 Continaud, M., Bonniau, P. and Bunsell, A. R. *J. Mater. Sci.* 1982, **17**, 867
- 6 Reid, J. D. and Lawrence, W. H. *J. Appl. Polym. Sci.* 1986, **31**, 1771
- 7 Woo, M. and Piggot, R. *J. Compos.* 1988, **10**, 16
- 8 Paquin, L., St-Onge, H. and Wertheimer, M. R. *IEEE Trans. Electr. Insul.* 1982, **EI-17** (5), 399
- 9 Pleuddemann, E. P. 'Silane Coupling Agents', Plenum Press, New York, 1982
- 10 Steeman, P. A. M. and Maurer, F. H. J. *Colloid. Polym. Sci.* 1990, **268**, 315
- 11 Maurer, F. H. J., Steeman, P. A. M. and van Es, M. A. Proc. ICCM, Vol. VII, 1989, 232
- 12 Bonniau, P. and Bunsell, A. R. *J. Compos. Mater.* 1981, **15**, 272
- 13 Maurer, F. H. J. 'Polymer Composites' (Ed. B. Sedlacek), de Gruyter, Berlin, 1986, 399
- 14 Maurer, F. H. J., Papazoglou, E. and Simha, R. 'Advanced Concepts of Interfaces in Polymer, Ceramic and Metal Matrix Composites', Vol. 2, (Ed. H. Ishida), Elsevier Scientific, Amsterdam, 1988, 747
- 15 Böttcher, C. J. F. and Bordewijk, P. 'Theory of Electric Polarization', Vol. II, Elsevier Scientific, Amsterdam, 1978
- 16 Beek, L. K. H. *Prog. Dielec.* 1967, **7**, 69
- 17 Cole, K. S. and Cole, R. H. *J. Chem. Phys.* 1941, **9**, 341
- 18 Fripiat, J. J. and Jelli, A. *J. Phys. Chem.* 1965, **69**, 2185